Influence of matrix microstructure and test conditions on the pseudoductile failure of CVI-CFC

R.Ermel, T.Beck, C.Fleck
Institute of Materials Science I, University of Karlsruhe
Kaiserstr. 12, D-76131 Karlsruhe
tilmann.beck@mach.uni-karlsruhe.de

Abstract

The pseudoductile behaviour of carbon fibre reinforced carbon (CFC) made by chemical vapour infiltration (CVI) is supposed to be controlled by the fibre-matrix interface and the matrix microstructure. The matrix texture is analysed with polarized light microscopy (PLM). For an investigation of the failure behaviour tensile tests with different strain rates on a bi-directionally reinforced (2D)-CFC material with two variations in matrix texture are carried out. A decreasing pseudoductility with increasing content of low-textured pyrocarbon in the matrix and increasing strain rate is obtained. SEM-examinations of the fracture surfaces show a similarity of both effects in the way that crack deflection at the interfaces between matrix and fibre or inside the matrix is reduced. Another consequence of higher strain rates is an increase of Young´s modulus, which seems to be similar to a viscoelastic behaviour. For a further investigation of the failure mechanisms stepwise loading-unloading tests are carried out.

1 Introduction

High strength at temperatures up to 1800°C predestinates CFC as a material for components which undergo extremely high thermal and mechanical loadings e.g. for aeronautics and space-technology. However, a prerequisite for these applications is a sufficient toughness of the material consisting of two brittle components: carbon fibre and matrix consisting of pyrolytic carbon.

This so called pseudoductile behaviour is possible if the fibre-matrix interface shows an appropriate strength. Then the fracture mechanism of the composite can be described as seen in Fig. 1: A crack inside the matrix deflects at the fibre-matrix interface, a locally limited debonding between fibre and matrix takes place and the fibre will bridge the crack. Additionally, fibre fracture during further loading can cause so-called fibre-pullout, consuming additional energy for crack propagation [1-3].
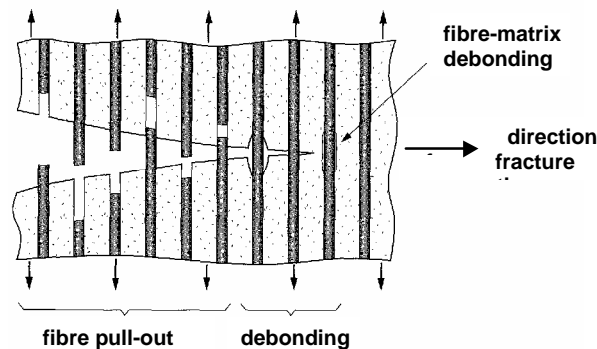
FIGURE 1. Failure behaviour of a unidirectionally reinforced pseudoductile composite [3].

Additionally the texture of the carbon matrix is important for the pseudoductile behaviour of CFC: On the one hand fibre-matrix bonding depends on the texture of the pyrolytic carbon. On the other hand fracture toughness can be further increased if crack deflection occurs in the matrix itself [4]. Especially high-textured matrix carbon, which is deposited in oriented, concentric layers around the fibre supports this behaviour.

This is proved by tests on chemical vapour infiltrated (CVI) fibre felts that show, that a material with a larger volume fraction of high textured matrix possesses a more pronounced pseudoductility than composites with medium or low textured matrices [5].

2 Experimental

2.1 Investigation of the microstructure

The investigation of the matrix texture is carried out by PLM on specimens cut perpendicular to the main fibre direction. The measurement of the extiction angle of polarized light characterizes the texture of pyrolytic carbon, so that a distinction between isotropic (ISO), low (LT), medium (MT) und high textured (HT) carbon is possible [6].

2.2 Mechanical testing and specimen geometry

Tensile tests are performed on an electromechanical testing machine. The integral strain is measured with a capacitive extensometer. Additionally an optical extensometer based on grey-scale-correlation analysis allows for an integral as well as a locally resolved determination of the strains [7]. The tests are carried out with constant crosshead velocities from 0.002 mm/min up to 20 mm/min. The determination of Young´s modulus at unloading is realized by force-controlled tests.

Because of the limited CVI-reactor dimensions the maximum specimen length is $L = 52$ mm. Their cross-section is $B \times H = 2 \times 3$ mm^2 and the gauge-length $L_0 = 15$ mm. Figure 2 shows the geometry of the tensile specimens.
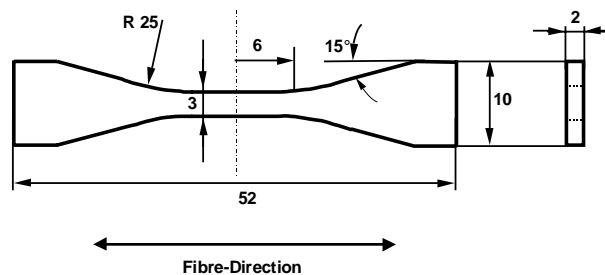
FIGURE 2. Geometry of the tensile specimens.

3 Materials

The investigated material consists of an infiltrated 2D fibre preform with a sequence of the plies in 0°/0°/90°/90° direction as seen in figure 3. The overall fibre content is $V_F = 22.5$ %. Between the plies a thin felt layer can be found. Within each ply, 80% of the fibres are oriented in the main direction. The specimens are taken from the infiltrated preform in such a way that the direction of the load-axis and fibres are parallel.

The material is produced by chemical vapour infiltration. During this process Methane diffuses into the fibre preform, where it cracks into hydrogen and elementary carbon which is

deposited on the surface of the fibres until the fibre structure is mainly densified. Because of an exact understanding of the CVI process [8, 9], it is possible to produce a composite of high density within a time of a few days.
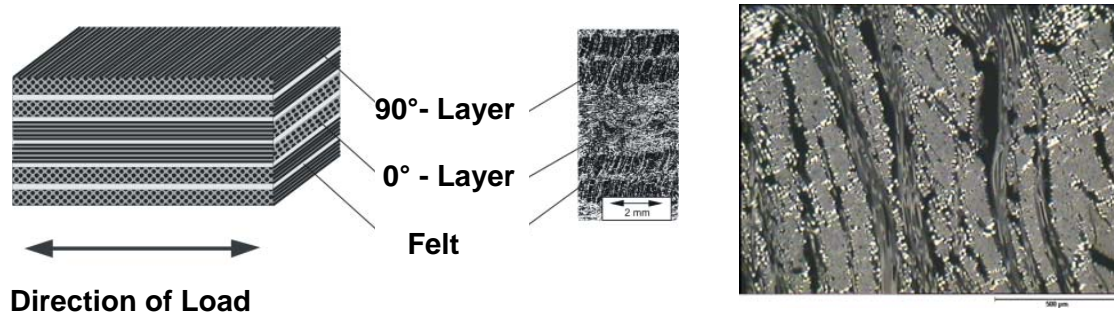
FIGURE 3: CVI-CFC material out of a 2D-0/0/90/90 fibre-preform (left), bundle structure of the used 2D-CFC material (right).

A polarized light micrograph (Fig. 3, right) shows the typical bundle structure of the investigated material. Two variations of this material are used for the investigations. The first was infiltrated at ICT, University of Karlsruhe, in the frame of the SFB 551 [9] and the second was manufactured by the Sintec Company.

Differences in density, porosity and texture of the matrix carbon can be recognized in Fig. 4 and are summarized in Table 1. Density, open porosity and texture are determined in the centre of the specimen, which is relevant for a correlation with mechanical properties.

TABLE 1. Material properties and texture of the investigated materials.

Rank	Origin	Mean density [g/cm³]	Mean porosity [%]	Texture of the matrix
Material 1	SFB	1,71	10,0 (9,0-11,0)	thick ring of LT+HT
Material 2	Sintec	1,73 (1,7-1,77)	12,0 (10,0–14,0)	thin ring of LT+HT

Both materials show two distinct textures in the matrix carbon: At first LT-carbon is deposited around the fibres but during further infiltration the texture changes into HT-carbon. In the case of material 1 the LT-carbon rings around the fibres are much thicker and within the HT-layers the texture seems to be a little bit sharper than in material 2 (Fig. 4).
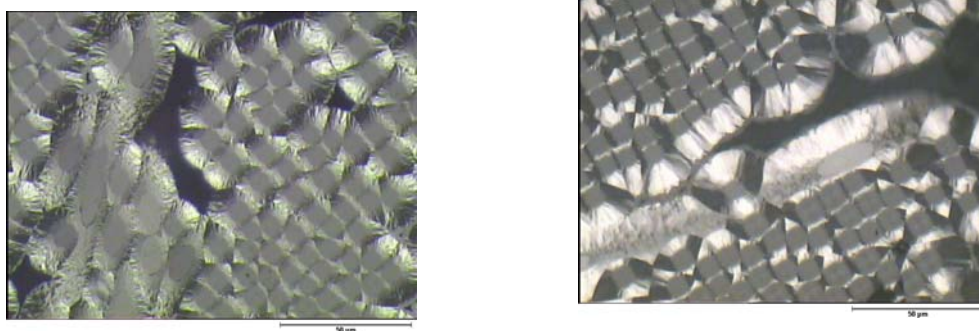
FIGURE 4. Polarized light micrographs of material 1 (left) and material 2 (right).

4 Results

4.1 Influence of matrix microstructure on the failure behaviour of CFC

As becomes obvious from Fig. 5, at intermediate strain rates the stress-strain curve for material 1, which possesses the larger LT-pyrocarbon layer around the fibres, shows a more brittle behaviour, whereas materials 2 has a more pronounced pseudoductility. Strength and Young´s-modulus of both materials are approximately the same. The scatter of mechanical properties is greater for material 1 due to the larger scatter of density and open porosity.
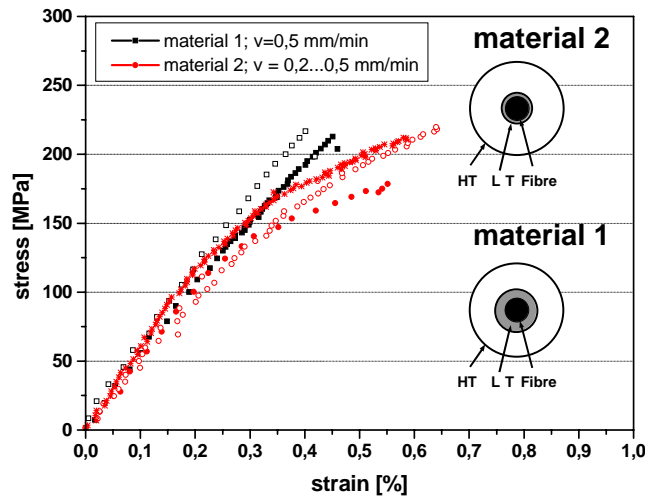
FIGURE 5. Stress-strain curves of both investigated materials.

In accordance with the mechanical behaviour, the fracture surface of material 1 is very smooth. It seems that a crack propagates through matrix and fibre without stopping at the interfaces (see arrow at Fig. 6, left). On the other hand the fracture surface of material 2 is much rougher and a little more fibre-pullout can be recognized.
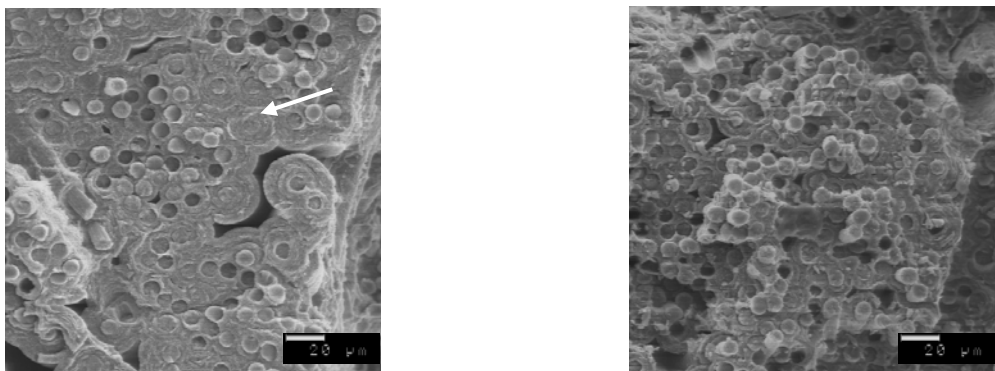
FIGURE 6. Fracture surfaces of material 1 (left) and material 2 (right).

4.2 Influence of the strain rate on fracture behaviour

Stress-strain curves of material 2 from tensile tests at different crosshead velocities of 20 mm/min, 0,2 mm/min and 0,002 mm/min are given in Fig. 7. An increase of the strain rate by four orders of magnitude results in a growth of Young´s modulus from 44 GPa to 72 GPa.

At the same time an increase of the strain rate leads to a distinct decrease of plastic fracture strain.
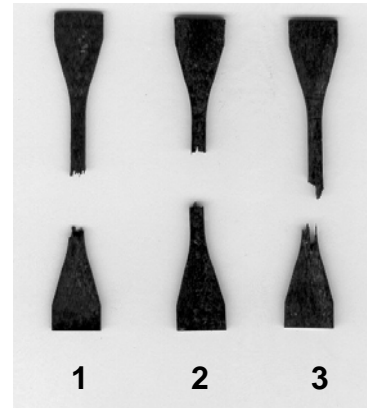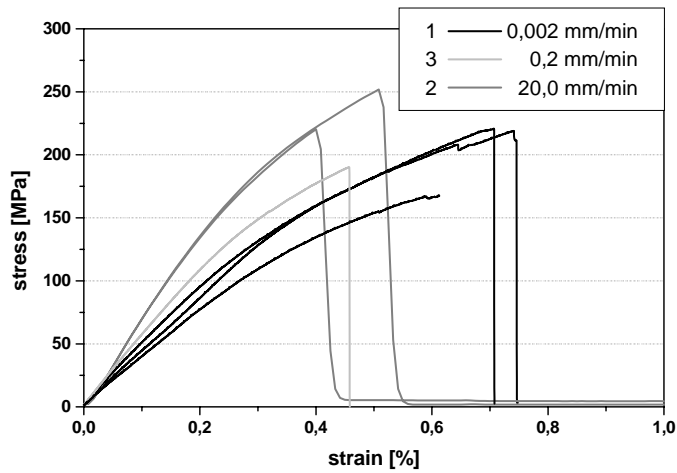
FIGURE 7. Stress-strain curves of material 2 from tensile tests at different strain rates (left) and fractured specimens tested with increasing strain rates (right).

In order to get a deeper understanding of the micromechanical processes inside matrix and at the fibre-matrix interface fractographic investigations were carried out. A first macroscopic view of the fractured test pieces is given in Fig. 7, right. The results seem to be untypical for conventional materials, because low strain rates, which lead to a more ductile behaviour result in a straight fracture path perpendicular to load direction, whereas the brittle failure at high strain rates apparently leads to a diagonal fracture. However, a closer view on the later sample showed a stepped fracture path.

SEM pictures of the fracture surfaces at different strain rates are given in Fig. 8 (left and middle). Samples undergoing a high strain rate show a relatively smooth fracture surface. In the case of low strain rates a more pronounced fibre-pullout can be detected. Accordingly, a grinding of the same sample in longitudinal direction revealed a crack bridged by a number of fibres, which did not lead to fracture (Fig.8, right).
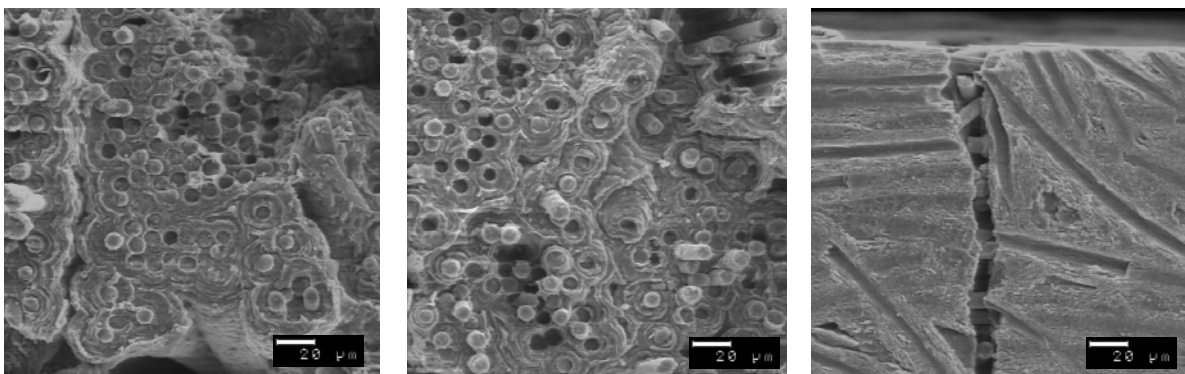
FIGURE 8. Scanning electron micrographs of specimens fractured at a crosshead velocity of 20 mm/min (left) and 0,002 mm/min (middle, right).

4.3 Young´s modulus at unloading

For a quantitative determination of the damage processes, tensile tests with stepwise loading and unloading are carried out for material 2. The resulting stress-strain curve of one sample shows a decreasing Young´s modulus with increasing load (Fig. 9, left). The presentation of Young´s modulus versus the applied stress results in a diagram as seen in Fig. 9, right. For all three samples investigated Young´s modulus begins to decrease up from a stress of $\sigma_n = 70$ MPa. The scatter of density and open porosity explains the differences of the absolute values of Young´s modulus.
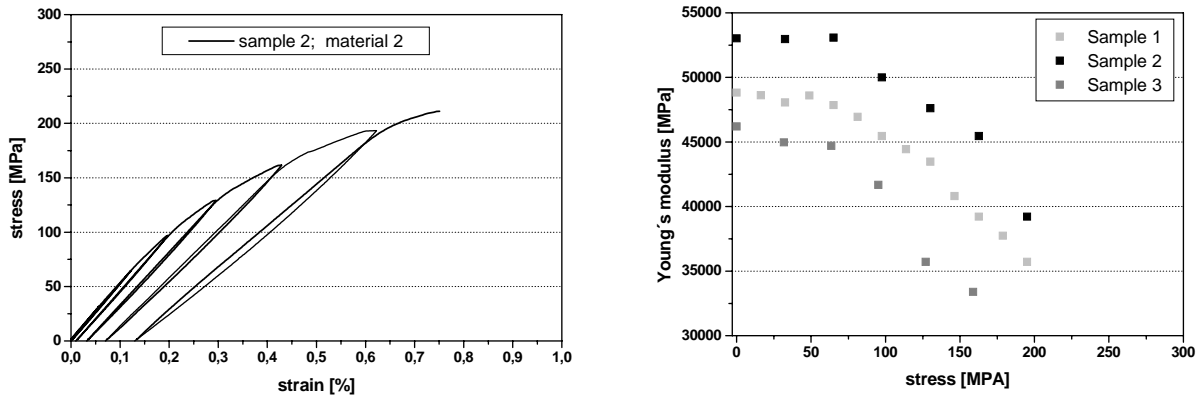
FIGURE 9. Typical stress-strain curves for stepwise loading and unloading tests of sample 2 (left), Young´s modulus-stress diagram for three samples of material 2 (right).

5 Discussion

A lower density and higher open porosity may cause an increasing pseudoductility of material 2 compared to material 1 as seen in Fig. 5. However, these effects seem to be not big enough to explain the distinct differences of the failure behaviour of both materials.

For a more detailed discussion, the different diameter of LT-pyrocarbon layer around the fibre has to be considered. The fibre and additionally the LT layer can be assumed as a virtual fibre (Fig. 10), which fails without delamination and therefore causes an increasingly brittle behaviour with increasing thickness [5]. Additionally the volume fraction of LT-carbon in the matrix is much higher for material 1 than for material 2. Especially the zones of high fibre density inside a fibre bundle hardly contain any hightextured carbon (Fig. 3). Therefore the possibility of crack deflection is reduced.
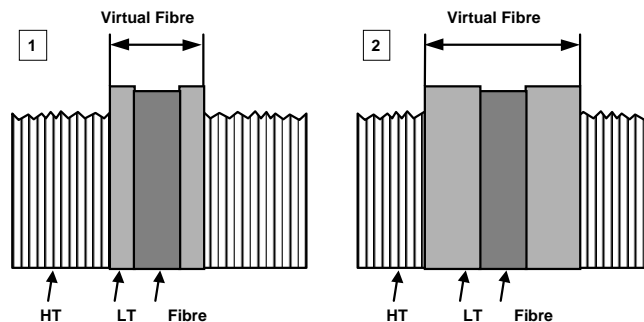
FIGURE 10. Virtual fibre of material 1 (right) and material 2 (left) [5].

The increase of Young´s modulus and the decrease in pseudoplasticity of the composite as the rate of deformation is increased (Fig. 7) is similar to a viscoelastic behaviour, although the responsible mechanisms must be different: Viscoelasticity is a time dependent and reversible deformation behaviour of materials, e.g polymers. In the case of CFC the deformation is caused by irreversible processes such as crack propagation.

The increase of pseudoplasticity with decreasing crosshead speed can be explained with the time dependence of the micromechanical processes inside the matrix and at the fibre-matrix interface. In the case of higher strain rates the decrease of the stress at the crack tip by crack deflection is not as pronounced as at low strain rates. Consequently, a propagating crack does not stop at fibre-matrix interfaces in the composite.

The fracture behaviour as seen in Fig. 7 may be interpreted using the surface strain distribution determined by optical extensometry (Fig. 11, right). At a state with an integral strain of $\varepsilon_t = 0.14$ %, the local strains of a specimen tested with low strain rates (2) lead to a comparatively uniform strain distribution, whereas a high crosshead speed (1) causes pronounced strain inhomogenities. It is assumed that in the latter case fracture is caused by a small number of large cracks which connect across different planes along weak regions in the composite e.g. pores (Fig. 11, left). In the case of a low strain rate (2) a large number of microcracks may be formed in the matrix. The straight fracture path then will be caused by a crack, which has enough time to propagate through matrix and by-pass the fibres. Because of the limited resolution of the optical extensometer strain distribution seems to be homogeneous.
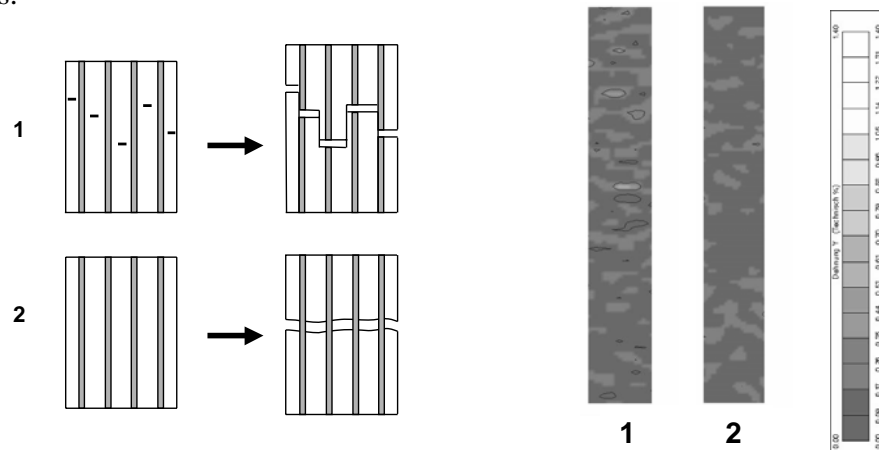
FIGURE 11.   Model for the failure behaviour (left), strain distribution out of optical extensometry (right) for v_{test} = 20 mm/min (1) and v_{test} = 0,002 mm/min (2).

However, the interpretation of the increase of Young´s modulus with increasing strain rate by the same mechanisms requires the assumption that even at the beginning of tests with low crosshead speed the whole matrix is cracked or debonding across the total area takes place.

For a quantitative analysis Young´s modulus of the composite is estimated from Young´s moduli of fibre E_F and matrix E_M as well as fibre content V_F using the rule of mixture (Eq. 1).

$$E = E_F \cdot V_F + E_M \cdot (1 - V_F) \tag{1}$$

At the lowest strain rates Young´s modulus is E = 44 GPa (Fig. 7, left). This is not much more than the value of E = 42,5 GPa which is the contribution of longitudinal fibre content of 18 % in the composite calculated with Eq. 1 assuming a Young´s modulus of E_F = 190 GPa for the fibre.

Due to the fact that at higher crosshead velocities larger Young´s moduli than resulting from the rule of mixture are observed, further research is planned to recognize the effects resulting in this behaviour.

6 Summary

CVI-CFC materials with 2D fibre-architecture and two different matrix microstructures are examined in tensile tests with the aim to investigate the mechanisms of pseudoductile failure.

In the case of a higher content of LT pyrocarbon within the matrix a less pseudoductile behaviour is recognized. This agrees with fractographic investigations in SEM, which show relatively smooth fracture surfaces. Increasing brittleness and Young´s modulus is observed when crosshead velocity increases. A smooth fracture surface with less fibre-pullout is recognized here, too.

In both cases of brittle fracture a reduced debonding between fibre and matrix or between different matrix layers is observed. The interpretation for the first case is that a fibre with a pronounced LT-carbon layer behaves like a thicker virtual fibre. The reason for the reduced pseudoductility with increasing strain rates is the time dependence of micromechanical processes. For a further examination of the fracture behaviour stepwise loading-unloading tests are carried out to investigate the development of damage in the composite. They show a decrease in Young´s modulus, i.e. the beginning of a damaging process, at a stress of about 70 MPa.

The reasons for the strain rate dependence of Young's Modulus which similar as a viscoelastic behaviour, will be examined in further tests.

Acknowledgement

References

1. Fitzer, E., Manocha, L.M., Carbon reinforcements and Carbon/Carbon Composites, Springer, Berlin Heidelberg, 1998.

2. Evans, A.G., Marshall, D.B., Acta Metall., 37, 2567-2583, 1989.

3. Berthelot, J.-M., Composite Materials, Springer, New York, 2000.

4. Reznik, B., Gerthsen, D., Carbon, 41, 57-69, 2003.

5. Reznik, B., Guellali, M., Gerthsen, D., Oberacker, R., Hoffmann, M. J., Mat. Letters, 52, 14-19, 2002.

6. Reznik, B., Hüttinger, K.J., Carbon, 40, 621-624, 2002.

7. GOM mbH, Aramis – Verformungsmessung nach dem Rasterverfahren, Aramis 4.7.3-2 (2002) , 5.2.0-2 (2003).

8. Hüttinger, K.J., Chem. Vap. Deposition, 4, 151-158 (1998).

9. Zhang, W.G., Hüttinger, K.J., Carbon, 41, 2325-2337, 2003.